

Title

Max Varverakis

May 4, 2024

# Contents

<b>1</b>	<b>Introduction</b>	<b>4</b>
<b>2</b>	<b>An Introduction to Representation Theory</b>	<b>4</b>
2.1	Irreducibility and Invariant Subspaces . . . . .	6
<b>3</b>	<b>Examples in Physics</b>	<b>8</b>
3.1	Rotations in a plane and the group $SO(2)$ . . . . .	8
3.1.1	The rotation group . . . . .	8
3.1.2	Infinitesimal rotations . . . . .	10
3.1.3	Irreducible representations of $SO(2)$ . . . . .	11
3.1.4	Multivalued representations . . . . .	13
3.1.5	State vector decomposition . . . . .	14
3.2	Continuous 1-dimensional translations . . . . .	16
3.2.1	Irreducible representations of $T_1$ . . . . .	18
3.2.2	Explicit form of $P$ . . . . .	18
3.2.3	Generalization to 3-dimensional space . . . . .	19
3.3	Symmetry, invariance, and conserved quantities . . . . .	20
3.3.1	Conservation of linear momentum . . . . .	21
3.3.2	Conservation of angular momentum . . . . .	22
3.4	3D rotations and the group $SO(3)$ . . . . .	23
3.4.1	Explicit form of $\mathbf{J}$ . . . . .	24
3.4.2	Commutation relations of $SO(3)$ generators . . . . .	25
3.4.3	Irreducible representations of $SO(3)$ . . . . .	26
3.5	Physical implications of $SO(3)$ . . . . .	29
3.5.1	Quantization of observables . . . . .	31
3.5.2	Additional applications . . . . .	32

<b>4</b>	<b>Topological Definitions</b>	<b>34</b>
<b>5</b>	<b>The Braid Group</b>	<b>37</b>
5.1	Visualization of pure braids . . . . .	37
5.2	General braids . . . . .	39
5.3	Standard generators of the braid group . . . . .	40
5.4	Automorphisms of the free group . . . . .	41
5.5	One-dimensional representations of $B_n$ . . . . .	46
5.6	The Burau Representation . . . . .	47
5.7	The Reduced Burau Representation . . . . .	52
5.8	Unitary Representation Matrices . . . . .	57
<b>6</b>	<b>Anyons</b>	<b>60</b>
6.1	Braiding action on a quantum system . . . . .	60
6.2	Two Non-Interacting Anyons . . . . .	62
6.3	Anyons in Harmonic Potential . . . . .	64
6.4	Nontrivial braiding effects . . . . .	66
<b>6</b>	<b>tikz test</b>	<b>68</b>
<b>7</b>	<b>To-Do List</b>	<b>69</b>
	<b>Bibliography</b>	<b>72</b>
<b>A</b>	<b>Physics Background</b>	<b>73</b>
A.1	Dirac notation . . . . .	73
A.2	Commutator Identities . . . . .	74
A.3	Commutation relations for $SO(3)$ . . . . .	75
A.4	Ehrenfest's theorem and conserved quantities . . . . .	75
<b>B</b>	<b>Multi-anyon system with harmonic potential</b>	<b>77</b>
B.1	Gauge Theory and the Hamiltonian . . . . .	77
B.2	Hamiltonian Terms . . . . .	77

# List of Figures

5.1	Pure braid . . . . .	38
5.2	General braid . . . . .	40
5.3	Artin generators . . . . .	41
5.4	Fundamental group of the punctured disk . . . . .	42
5.5	Artin generators realized on the punctured disk . . . . .	43
5.6	Graphical verification of Eqn. 5.3 . . . . .	44
5.7	Graphical verification of Eqn. 5.6 . . . . .	46
5.8	Punctured disk covering space . . . . .	49
5.9	Covering space loop . . . . .	51
6.1	Anyon trajectories . . . . .	67

# Chapter 1

## Introduction

This is an introduction. Introduce the topic and general outline of the thesis.

## Chapter 4

# Topological Definitions

The braid group is formally defined in terms of topology. In order to understand the braid group, we must first understand the underlying topological properties that are used to define the braid group. Similar to an isomorphism in algebra, we can define a notion of equivalence in topology.

**Definition 4.1.** Consider  $X$  and  $Y$  to be two topological spaces. A *homotopy* between two continuous functions  $f, g : X \rightarrow Y$  is a continuous function  $H : X \times [0, 1] \rightarrow Y$  such that  $H(x, 0) = f(x)$  and  $H(x, 1) = g(x)$  for all  $x \in X$ . If such a homotopy exists, we say that  $f$  and  $g$  are *homotopic*.

The homotopy  $H$  can be thought of as a continuous deformation of  $f$  into  $g$ . The interval  $[0, 1]$  represents the “time” parameter of the deformation. At time equal to 0, the function  $H$  is equal to  $f$ , and at time equal to 1, the function  $H$  is equal to  $g$ . If two functions are homotopic, then they belong to the same homotopy class, which is an equivalence class of functions under the relation of homotopy.

**Definition 4.2.** A *loop* on a topological space  $X$  is a continuous function  $\ell : [0, 1] \rightarrow X$  such that  $\ell(0) = \ell(1)$ . In other words, the path of  $\ell$  starts and ends at the same point in  $X$ . Often, this point is called the *base point* of the loop.

**Definition 4.3.** A *homotopy class of loops* on a topological space  $X$  is an equivalence class of loops under the relation of homotopy. More plainly, a homotopy of loops is a continuous transformation of one loop into another.

If two loops  $\ell_1, \ell_2 : [0, 1] \rightarrow X$  with base point  $\xi \in X$  are homotopic, then there exists a continuous map  $H : [0, 1] \times [0, 1] \rightarrow X$  such that:

1.  $H(0, t) = \xi = H(1, t)$  for all  $t \in [0, 1]$ , and
2.  $H(s, 0) = \ell_1(s)$  and  $H(s, 1) = \ell_2(s)$  for all  $s \in [0, 1]$ .

Property 1 ensures that the starting/ending point of the loop remains fixed throughout the deformation from  $\ell_1$  to  $\ell_2$ , and property 2 follows from the definition of a homotopy.

**Definition 4.4.** The *fundamental group* of a topological space  $X$  with base point  $\xi$  is defined as the collection of loops on  $X$  with base point  $\xi$  modulo homotopy. In other words, the fundamental group is the collection of equivalence classes of loops under homotopy. This is written as

$$\pi(X, \xi) := \{\text{loops } \ell \text{ on } X \text{ with base point } \xi\} / \text{homotopy}.$$

Often times, the base point of a loop is arbitrary, so we can write  $\pi(X)$  instead of  $\pi(X, \xi)$  to denote the fundamental group of  $X$ .

The group structure of the fundamental group is defined as operations on the loops themselves. Consider two loops  $\ell_1, \ell_2 : [0, 1] \rightarrow X$  with base point  $\xi$ . Then the product  $\ell_1 \cdot \ell_2$  is defined in terms of *concatenation* of the two loops. Specifically, this defines a new loop  $(\ell_1 \cdot \ell_2)(t) = \mathcal{L}(t) : [0, 1] \rightarrow X$  where  $\mathcal{L}(t) = \ell_1(2t)$  on  $[0, \frac{1}{2}]$  and  $\mathcal{L}(t) = \ell_2(2t - 1)$  on  $[\frac{1}{2}, 1]$ . Loop concatenation can be thought of as stitching the loops together at the shared base point. As  $t$  ranges from 0 to 1, we can think of the first half of the deformation as traversing the first loop at twice the original speed, and then traveling along the second loop at twice the original speed in the second half of the deformation.

In the above description, recall that each loop  $\ell$  is actually an equivalence class  $[\ell]$  under the relation of homotopy. So the concatenation of two loops  $\ell_1$  and  $\ell_2$  is actually the concatenation of any two loops belonging to the equivalence classes  $[\ell_1]$  and  $[\ell_2]$ , which becomes the equivalence class  $[\ell_1 \cdot \ell_2]$ .

In the fundamental group, the inverse of an element is the identical topological path traversed in the opposite direction. Hence, if  $\gamma : [0, 1] \rightarrow X$  is a loop on  $X$ , then  $\gamma^{-1}(t) := \gamma(1 - t)$ .

Just as how homotopy describes a continuous transformation from one continuous path on a topological space to another, we can define topological

equivalence on a larger scale.

**Definition 4.5.** A continuous, bijective function  $f : X \rightarrow Y$  between two topological spaces  $X$  and  $Y$  such that the inverse  $f^{-1} : Y \rightarrow X$  is also continuous and bijective is called a *homeomorphism*. If there exists such a homeomorphism, then we say  $X$  is *homeomorphic* to  $Y$ . Moreover, an *embedding* of topological spaces is a continuous function that is a homeomorphism when restricted to its image. If we have a continuous family of homeomorphisms  $f_t : X \rightarrow Y$  for  $t \in [0, 1]$ , then we say that  $X$  and  $Y$  are *isotopic*. The isotopy of  $X$  and  $Y$  can be written as a function  $H : X \times [0, 1] \rightarrow Y$  such that

1.  $H(x, 0) = x$  for all  $x \in X$ ,
2.  $H(x, 1) = f(x)$  for all  $x \in X$ , and
3.  $H(-, t)$  is an embedding of  $X$  onto  $Y$  for all  $t \in [0, 1]$ .

Evidently, isotopy defines a stronger and more broad notion of topological equivalence, which will be important in defining representations later on.



# Chapter 5

## The Braid Group

**Definition 5.1.** The *configuration space* of  $n$  ordered distinct points in the complex plane  $\mathbb{C}$  is defined as  $M_n = \{(z_1, \dots, z_n) \in \mathbb{C}; z_i \neq z_j, \forall i \neq j\}$ . Alternatively, consider  $\mathcal{D}$  to be the collection of all hyperplanes  $H_{i,j} = \{z_i = z_j\} \in \mathbb{C}^n$  for  $1 \leq i < j \leq n$ . Then we can define  $M_n = \mathbb{C}^n \setminus \mathcal{D}$ .

Note that  $(z_1, z_2, z_3, \dots, z_n)$  and  $(z_2, z_1, z_3, \dots, z_n)$  are different points in the configuration space  $M_n$ . Before studying the various interpretations of the braid group, we first define the braid group itself.

**Definition 5.2.** The *pure braid group* on  $n$  strands, denoted  $PB_n$ , is the fundamental group of  $M_n$ . One can write  $PB_n = \pi_1(M_n)$ .

### 5.1 Visualization of pure braids

We can think of a pure braid as a loop in  $M_n$ :

$$\begin{aligned} \beta : [0, 1] &\rightarrow M_n \\ t &\mapsto \beta(t) = (\beta_1(t), \beta_2(t), \dots, \beta_n(t)), \end{aligned}$$

with some base point. Conventionally, we define the base point as the  $n$ -tuple of integers  $(1, 2, 3, \dots, n) \in \mathbb{C}^n$ . Then a pure braid can be thought of the motion of these points in the complex plane as  $t$  ranges from 0 to 1 in which  $\beta_i(t)$  is defined and  $\beta_i(t) \neq \beta_j(t)$  for every  $t \in [0, 1]$  and  $i \neq j \in \{1, 2, \dots, n\}$ . Because each  $\beta_i$  is a loop, it must start and end at the point

$i$  (e.g.,  $\beta_i(0) = \beta_i(1) = i$ ). Recall that the loops are actually equivalence classes of loops under homotopy. As a result, we can continuously deform the motion of the  $n$  points while maintaining the same pure braid (up to equivalence) so long as we preserve the pairwise distinction of the points for all time  $t \in [0, 1]$ .

A common visualization of pure braids is to plot the motion of the points in 3-dimensional space. For each  $t \in [0, 1]$ , we draw the points  $(\beta_i(t), t)$  in  $\mathbb{C} \times [0, 1]$  for every  $i \in \{1, \dots, n\}$ . The space  $\mathbb{C} \times [0, 1]$  can be thought of as a spacetime diagram, where the motion of the points is plotted in the complex plane at each time  $t$ , with the time being the vertical axis. The convention is to have  $\mathbb{C} \times \{0\}$  placed above  $\mathbb{C} \times \{1\}$ , so that the motion of the points is plotted from top to bottom, as in Figure 5.1.

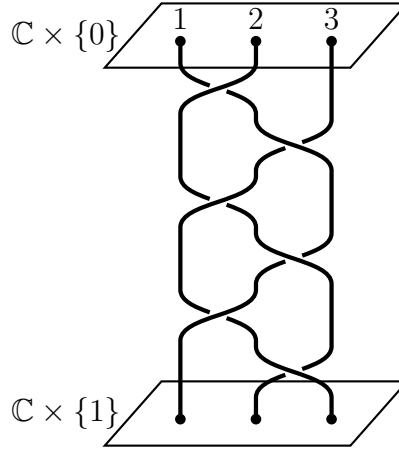


**Figure 5.1:** A pure braid on three strands is visualized as the trajectory of three particles as they move in  $\mathbb{C}$ , plotted over an arbitrary (normalized) time period. Each point ends at the same relative starting position in  $\mathbb{C}$ .

For every  $i \in \{1, \dots, n\}$ , the motion of a single point starting at  $(i, 0)$  and ending at  $(i, 1)$  is known as the  $i$ -th *strand* of the pure braid. This can also be described by the  $i$ -th projection of the  $n$ -tuple  $\beta(t)$ . Thus, two braids are equivalent under homotopy if, for every moment of a continuous deformation of the  $n$  strands in  $\mathbb{C} \times [0, 1]$ , the (fixed) endpoints  $((1, 0), (2, 0), \dots, (n, 0))$  and  $((1, 1), (2, 1), \dots, (n, 1))$  are connected by strands that are pairwise disjoint where each strand intersects the plane  $\mathbb{C} \times \{t\}$  exactly once for every  $t \in [0, 1]$ .

As pure braids are members of the pure braid group, multiplication is a well-defined operation. In the context of  $M_n$ , multiplication of pure braids involves the concatenation of loops. Visually, this is the process of stacking braids on top of each other, and then rescaling the time dimension so that  $t$  ranges from 0 to 1.

## 5.2 General braids

In the previous section, we defined pure braids in which the endpoints of each strand are identical at the beginning and end of the motion. This notion generalizes to define (non-pure) braids. First, we define a more general configuration space than  $M_n$ . The symmetric group  $S_n$  permutes the  $n$  distinct points in  $\mathbb{C}$ . Then the *configuration space of  $n$  unordered points in  $\mathbb{C}$*  is the quotient space  $N_n = M_n/S_n$ .

**Definition 5.3.** The braid group on  $n$  strands is the fundamental group of  $N_n$ , denoted  $B_n = \pi_1(N_n)$ .

The visualization of a braid is the same as in the case of pure braids, only now the endpoints of each strand do not necessarily match the starting points, as illustrated Figure 5.2. For example, the  $i$ -th strand may start at the point  $(i, 0)$  but end at the point  $(j, 1)$  for  $i, j \in \{1, \dots, n\}$ . The equivalence of strands is still defined as before under the homotopy of loops. Loop concatenation defines the multiplication of braids, as before.

Note that for  $n \geq 1$  there is a natural inclusion  $\iota : B_n \hookrightarrow B_{n+1}$  in which we add a new strand to any  $\beta \in B_n$  that does not interact with the other strands.

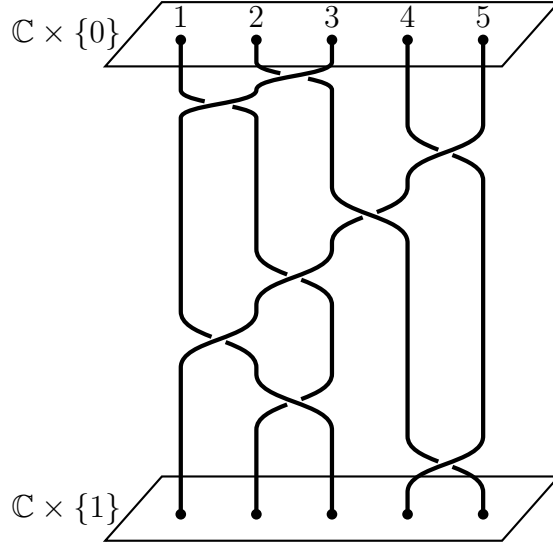


**Figure 5.2:** A general braid on five strands. The ending position of each particle is not necessarily in the same location of  $\mathbb{C}$  as the starting position, which classifies this as a general braid.

### 5.3 Standard generators of the braid group

Originally proposed by Artin [1], each braid can be decomposed into a product of *standard generators* of the braid group. When visualizing braids in  $\mathbb{R} \times [0, 1]$ , a crossing of two strands is clearly indicated by one going over the other, as in Figure 5.3. Suppose each crossing occurs at a different time  $t \in [0, 1]$ . Then by rescaling the time component of an arbitrary braid, we can decompose it into a stack of simple braids with only one crossing between neighboring strands per braid. Each single crossing of strands can be obtained by performing a transposition between neighboring endpoints of the strands.

For instance, swapping the endpoints of the  $i$ -th and  $(i+1)$ -th strands can be written as applying  $\sigma_i$  to the identity braid (i.e., the braid that starts without any crossings of strands). It must be noted that there are two distinct ways to swap the endpoints of two strands. From a top-down perspective looking at the plane  $\mathbb{C} \times \{t\}$  for some time  $t$ ,  $\sigma_i$  swaps  $(i, t)$  and  $(i+1, t)$  in a clockwise rotation. The reverse of this operation (i.e., twisting the endpoints around in the counterclockwise direction) is denoted  $\sigma_i^{-1}$ . Both of these operations are

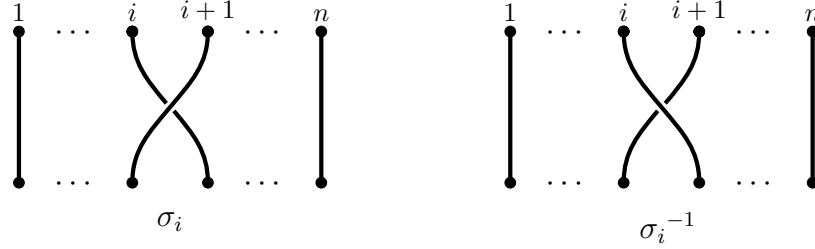


**Figure 5.3:** The action of  $\sigma_i$  on  $n$  strands. The  $i$ -th strand gets twisted behind the  $(i + 1)$ -th strand when acted on by  $\sigma_i$ , and the opposite occurs for  $\sigma_i^{-1}$ . In that way, concatenating these two braids would result in no intertwining of strands, giving the identity braid.

illustrated in Figure 5.3. The standard generators of the braid group  $B_n$  are defined as the set  $\{\sigma_1, \sigma_2, \dots, \sigma_{n-1}\}$ . An arbitrary braid can be constructed by concatenating (or stacking) the simple braids made from the standard generators before rescaling the time coordinate to  $[0, 1]$ .

A general braid can be written as a product of the standard generators and their inverses. One of the many metrics to characterize a braid involves the powers of the standard generators in its decomposition, as defined below.

**Definition 5.4.** The *degree* of a braid  $\beta \in B_n$  is the sum of the powers of the standard generators in the decomposition of  $\beta$ .

## 5.4 Automorphisms of the free group

Consider the  $n$ -times punctured disk  $\mathbb{D}_n$ . The fundamental group of  $\mathbb{D}_n$  involves loops that start and end at the same (fixed) base point in  $\partial\mathbb{D}_n$ . Up to homotopy, a clockwise-directional loop that encompasses the  $i$ -th hole in  $\mathbb{D}_n$  corresponds to the  $i$ -th generator of the free group  $F_n$  of rank  $n$ , which is illustrated in Figure 5.4. In fact,  $\pi_1(\mathbb{D}_n) = F_n$ . This equality allows us to define a representation of the braid group on  $n$  strands as automorphisms of  $F_n$ .

Each braid  $\beta \in B_n$  is realized as an automorphism of  $\pi_1(\mathbb{D}_n) = F_n$  (up to isotopy) where each loop  $\gamma \in \pi_1(\mathbb{D}_n)$  is sent to another loop  $\beta(\gamma)$ . In other

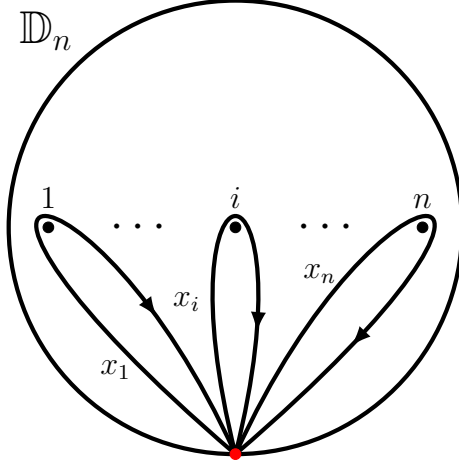


**Figure 5.4:** For each  $i \in \{1, \dots, n\}$ , the clockwise-directional loop encircling the  $i$ -th hole in  $\mathbb{D}_n$  corresponds to the  $i$ -th free generator of  $F_n$  (i.e.,  $x_i$ ). The red dot indicates the (arbitrary) base point for the loops in  $\pi_1(\mathbb{D}_n)$ .

words, we have a representation of the braid group defined by

$$\rho : B_n \rightarrow \text{Aut}(F_n) \quad (5.1)$$

$$\beta \mapsto \rho_\beta. \quad (5.2)$$

The action of  $\beta$  on a loop  $\gamma$  is defined by the rearrangements of the  $n$  holes in  $\mathbb{D}_n$ , similar to the action of the standard generators of  $B_n$  on the base points in  $\mathbb{C} \times \{1\}$ . In terms of the standard generators of  $B_n$ , each  $\sigma_i$  corresponds to switching the places of hole  $i$  and hole  $i+1$  by means of a clockwise rotation, as seen in Figure 5.5. This is identical to viewing the action of  $\sigma_i$  on the base points (Section 5.3) from above, looking down on the  $\mathbb{C} \times \{t\}$ -plane. As before, the inverse action  $\sigma_i^{-1}$  is a counterclockwise rotation of the two adjacent holes  $i$  and  $i+1$  in  $\mathbb{D}_n$ . These actions respect the group operation of loop concatenation.

Note that there is not a widely accepted convention for the standard generators of the braid group. For example, many sources will define the direction of the standard generators to be counterclockwise, where the punctures on  $\mathbb{D}_n$  are swapped in the opposite manner as in this thesis. Moreover, when considering the braid group as the intertwining of strands in  $\mathbb{C} \times [0, 1]$ , a generator  $\sigma_i$  may be defined as overlaying the  $i$ -th strand in front of the  $(i+1)$ -th

strand rather than behind. This is a matter of convention, and the choice of the standard braid permutations is equivalent up to inverses.

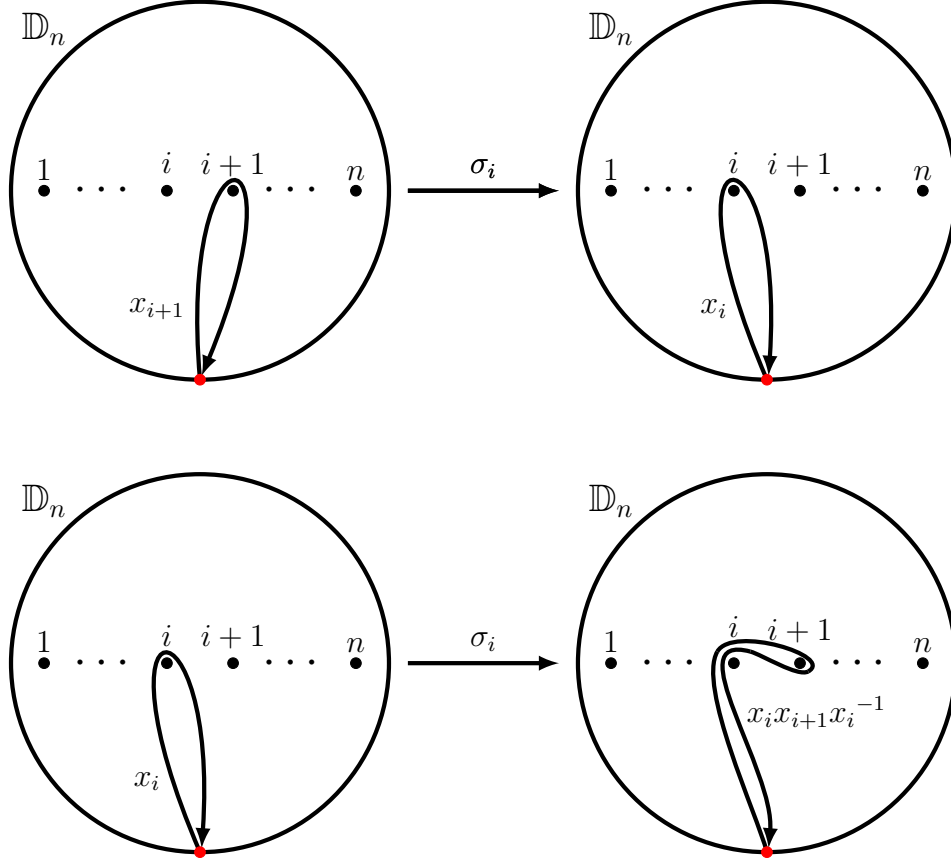


**Figure 5.5:** The action of  $\sigma_i$  on the generators  $x_i$  and  $x_{i+1}$  as described by Eqns. 5.3–5.5. The image of  $x_i$  under  $\sigma_i$  is verified visually in Figure 5.6

The automorphism  $\rho_\beta$  is most simply defined in terms of the action of the standard generators of  $B_n$  on the generators  $x_1, \dots, x_n$  of  $F_n$  (visualized as loops in  $\mathbb{D}_n$ ). For each  $i$ , it follows that

$$\rho_{\sigma_i}(x_i) = x_i x_{i+1} x_i^{-1}, \quad (5.3)$$

$$\rho_{\sigma_i}(x_{i+1}) = x_i, \quad (5.4)$$

$$\rho_{\sigma_i}(x_j) = x_j, \text{ for } j \neq i, i-1. \quad (5.5)$$

Clearly, any two loops that are separated by at least one puncture will not

interact while performing  $\sigma_i$ . The relations for adjacent loops can be verified graphically as illustrated in Figures 5.5 and 5.6.

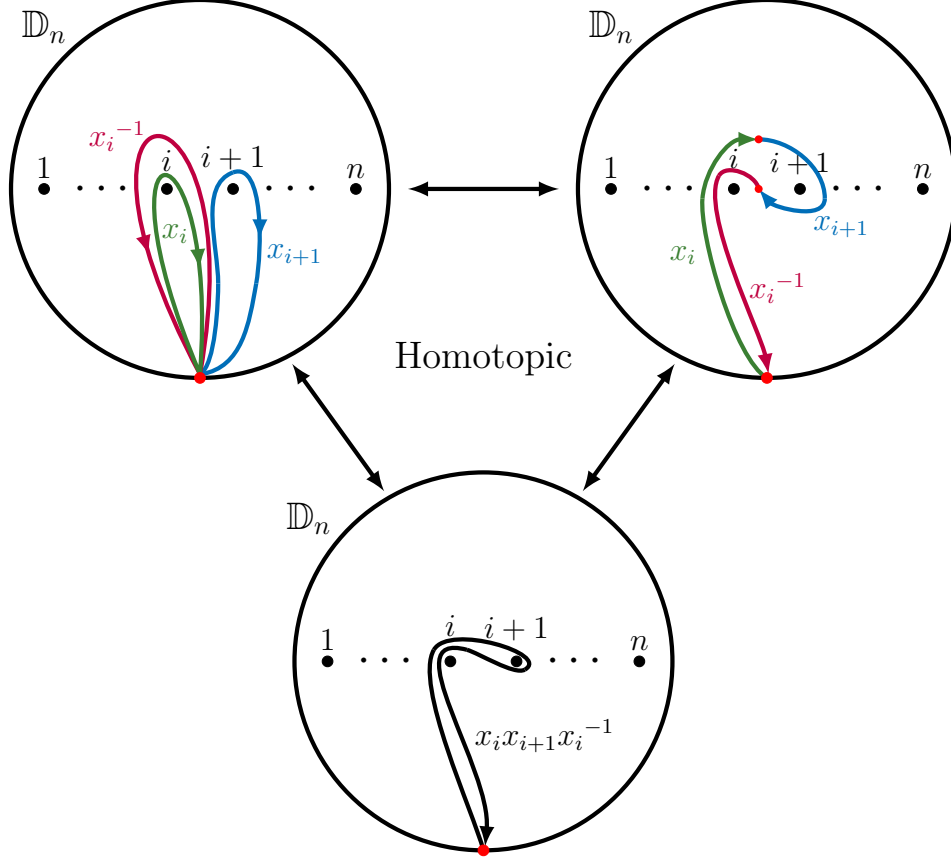


**Figure 5.6:** Up to homotopy, the product  $x_i x_{i+1} x_i^{-1}$  is visualized as the concatenation of the loops  $x_i, x_{i+1}, x_i^{-1} \in \pi_1(\mathbb{D}_n)$ . In the top right diagram, small red dots are used indicate the (homotopically deformed) points of concatenation.

For any  $\sigma_i$ ,  $\rho_{\sigma_i^{-1}}$  is well-defined. It follows that for any braid  $\beta \in B_n$ , we can decompose  $\rho_\beta$  the composition of the automorphisms of the standard generators  $\sigma_1, \dots, \sigma_{n-1}$  and their inverses that make up  $\beta$ .

Notice that for any  $\sigma_i$ ,  $\rho_{\sigma_i}(x_1 \cdots x_n) = x_1 \cdots x_n$ . This is because the loop  $x_1 \cdots x_n$  in  $\mathbb{D}_n$ , encompassing all holes, is parallel to the boundary  $\partial \mathbb{D}_n$ . Thus, the action of  $\sigma_i$  on  $x_1 \cdots x_n$  is trivial does not affect the structure of the loop



up to isotopy. More generally, this implies that  $\rho_\beta(x_1 \cdots x_n) = x_1 \cdots x_n$  for any  $\beta \in B_n$ . Paired with the observation that every generator is conjugate to another, Artin [1] showed that this is a necessary and sufficient condition for  $\rho_\beta$  to be an automorphism of  $F_n$ .

**Theorem 5.1.** *An automorphism  $f \in \text{Aut}(F_n)$  is equal to  $\rho_\beta$  for some  $\beta \in B_n$  if and only if*

1.  $f(x_i)$  is a conjugate of some  $x_j$  for every  $i \in \{1, \dots, n\}$ , and
2.  $f(x_1 \cdots x_n) = x_1 \cdots x_n$ .

In this interpretation of the braid group, we can express  $B_n$  in terms of the standard generators:

$$B_n = \left\langle \sigma_1, \dots, \sigma_{n-1} \left| \begin{array}{ll} \sigma_i \sigma_j = \sigma_j \sigma_i, & |i - j| > 1 \\ \sigma_i \sigma_{i+1} \sigma_i = \sigma_{i+1} \sigma_i \sigma_{i+1}, & |i - j| = 1 \end{array} \right. \right\rangle. \quad (5.6)$$

The first condition that the standard generators commute if  $|i - j| > 1$  is easily verified by thinking about the action of the generators on  $\pi_1(\mathbb{D}_n)$  as in Figure 5.5 and as automorphisms in Eqn. 5.5. This follows from the fact that if punctures  $i$  and  $j$  are non-adjacent, then the actions of  $\sigma_i$  and  $\sigma_j$  are mutually exclusive and thus commutative. The second condition on the standard generators is most easily verified in Figure 5.7 by looking at the corresponding braids in  $\mathbb{R} \times [0, 1]$  (here, the distinction between  $\mathbb{R}$  and  $\mathbb{C}$  is only a matter of choosing to show the starting and ending complex planes in traditional braid visualizations).

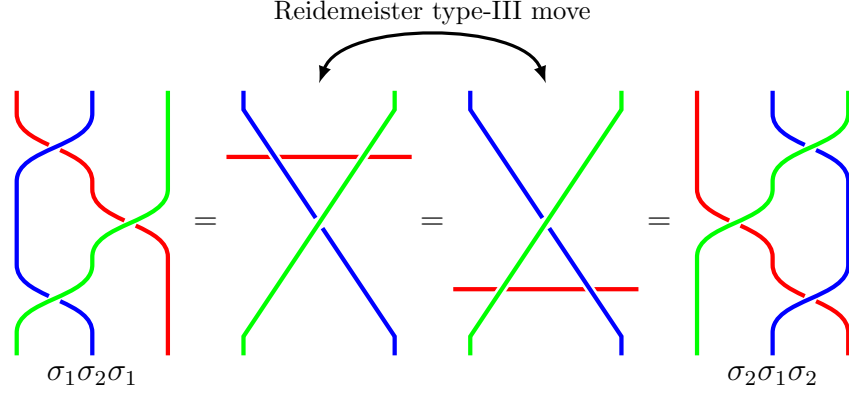


**Figure 5.7:** Graphical verification of Eqn. 5.6. All of the above braids are equivalent up to homotopy. The transformation between the middle two braid diagrams is known as a Reidemeister type-III move, in which the red strand (or string in the context of knot theory) is moved completely under the crossing of the blue and green strands. In these middle two diagrams, the red strand is slightly translucent to indicate that it is behind all other strands in the diagram.

## 5.5 One-dimensional representations of $B_n$

A straightforward nontrivial representation of the braid is defined on the standard generators of  $B_n$  and is given by [4]:

$$p_\theta : B_n \rightarrow \mathbb{C}_{|z|=1} \quad (5.7)$$

$$\sigma_i \mapsto e^{i\theta}, \quad (5.8)$$

for  $\theta \in \mathbb{R}$ . Clearly,  $p_\theta$  is a homomorphism, and it is unitary because

$$p_\theta(\sigma_i)^\dagger = (e^{i\theta})^\dagger = e^{-i\theta} = (e^{i\theta})^{-1} = p_\theta(\sigma_i)^{-1}, \quad (5.9)$$

where  $^\dagger$  denotes the conjugate transpose of a matrix.

Due to the abelian nature of the one-dimensional representations, we are free

to simplify products of braids. For example,

$$\begin{aligned}
p_\theta(\sigma_1\sigma_2\sigma_i^{-1}\sigma_2) &= p_\theta(\sigma_1)p_\theta(\sigma_2)p_\theta(\sigma_i^{-1})p_\theta(\sigma_2) \\
&= e^{i\theta_1}e^{i\theta_2}e^{-i\theta_1}e^{i\theta_2} \\
&= e^{i(\theta_1-\theta_1+\theta_2+\theta_2)} \\
&= e^{i\cdot 2\theta_2} = p_\theta(\sigma_2^2),
\end{aligned}$$

where the subscripts on  $\theta$  are only used to keep track of the contributing generator to each multiple of  $\theta$ . Hence, for a general braid  $\beta \in B_n$ , we can express  $p_\theta(\beta)$  as a simplified product of the standard generators of  $B_n$ :

$$p_\theta(\beta) = p_\theta(\sigma_1^{m_1}\sigma_2^{m_2}\cdots\sigma_{n-1}^{m_{n-1}}) = e^{i\theta(m_1+m_2+\cdots+m_{n-1})} = e^{ik\theta},$$

where  $k$  can be thought of as the degree of the braid.

Notice that with a choice of  $\theta = 2\pi n$  for  $n \in \mathbb{Z}$ , we recover the trivial representation of  $B_n$ . Similarly,  $p_{\pi n}$  is a restriction of the sign representation of  $S_n$ , where the sign of a permutation is defined as the parity of the number of transpositions in its decomposition into a product of transpositions.

## 5.6 The Burau Representation

In Section 5.4, we defined a representation of the braid group  $B_n$  as automorphisms of the free group  $F_n$ . This representation is clearly nonabelian. Likewise, the Artin generators of  $B_n$  are nonabelian. Suppose we wish to abelianize the braid group. The details of the abelianization of  $B_n$  would require a quotient by the commutator  $[a, b] = aba^{-1}b^{-1}$ .

Sparing the details, let  $B_{n,ab} = B_n/[B_n, B_n]$  be the abelianization of  $B_n$ , where  $[B_n, B_n] = \{[\beta_1, \beta_2] \mid \beta_1, \beta_2 \in B_n\}$  is the commutator subgroup of  $B_n$ . Then, under the representation  $\rho$  from Section 5.4, the abelianization of Eqns. 5.3–5.5 become

$$x_i \xrightarrow{\sigma_i} \cancel{x_i} + x_{i+1} - \cancel{x_i} = x_{i+1} = \rho_{\sigma_i^{-1}}(x_i), \quad (5.10)$$

$$x_{i+1} \xrightarrow{\sigma_i} x_i, \quad (5.11)$$

$$x_j \xrightarrow{\sigma_i} x_j, \text{ for } j \neq i, i-1, \quad (5.12)$$

for each  $i$ . Thus, the generator  $\sigma_i = \sigma_i^{-1}$ , and corresponds to a transposition permutation in the symmetric group  $S_n$ . It follows that  $B_{n,ab} \simeq S_n$ . In this

current construction, the abelianization of the braid group results in a loss of complexity. This raises the question whether there exists such a reframing of the braid group that allows an abelian operation on the free generators while preserving the inequivalence of the Artin generators with their inverses.

First, we define a topological space that will aid in the desired construction.

**Definition 5.5.** Let  $X$  be a topological space. A *covering* of  $X$  is a space  $\tilde{X}$  together with a continuous map  $p : \tilde{X} \rightarrow X$  such that, for every  $x \in X$ , there exists a path-connected open neighborhood  $U$  containing  $x$  such that  $p^{-1}(U)$  is a disjoint union of open sets in  $\tilde{X}$  where each component of  $p^{-1}(U)$  is mapped homeomorphically onto  $U$  by  $p$ . Each component of  $p^{-1}(U)$  is called a *sheet* of the covering, where the  $i$ -th sheet is denoted by  $\tilde{X}_i$ , and total the number of sheets in  $p^{-1}(U)$  is called the *degree* of the covering.

**Example 5.1.** One of the simplest examples of a covering space is the covering of the circle  $S^1$  by the real line by the parameterization map  $p : \mathbb{R} \rightarrow S^1$  defined by  $p(t) = (\cos t, \sin t)$ . Clearly, there are infinitely many sheets in this covering.

**Example 5.2.** A similar example is the covering of the circle  $S^1$  through  $p : [0, 1] \rightarrow S^1$  defined by  $p(t) = e^{2\pi it}$ . This defines a one-degree covering of  $S^1$ . If we instead let our domain be  $[0, 2]$ , then we have a two-degree covering of  $S^1$ .

With this topological tool, we construct a countably infinite-degree covering of the punctured disk  $\mathbb{D}_n$ , denoted  $\tilde{\mathbb{D}}_n$ , which can be visualized as an infinite stack of copies of  $\mathbb{D}_n$ , with a slight modification to be explained shortly. Let  $\tilde{\mathbb{D}}_{n,i}$  denote the  $i$ -th sheet of  $\tilde{\mathbb{D}}_n$ , and consider the base sheet our covering to be  $\tilde{\mathbb{D}}_{n,0}$ .

We start this construction with a countably infinite stack of copies of  $\mathbb{D}_n$ . Then, for every  $i \in \mathbb{Z}$ , for each of the  $n$  punctures on  $\tilde{\mathbb{D}}_{n,i}$ , apply a cut from the hole to some point on the boundary of  $\tilde{\mathbb{D}}_{n,i}$ , as illustrated in Figure 5.8 for the case when  $n = 3$ . Each cut results in two edges, which will be referred to as the left edge and the right edge. Through a homeomorphic deformation, connect the left edge of  $\tilde{\mathbb{D}}_{n,i}$  to the corresponding right edge of  $\tilde{\mathbb{D}}_{n,i+1}$ , and the right edge of  $\tilde{\mathbb{D}}_{n,i}$  to the left edge of  $\tilde{\mathbb{D}}_{n,i-1}$ , for every cut on every sheet.

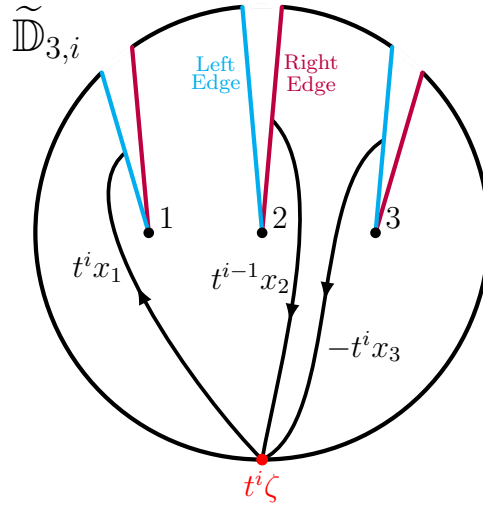


**Figure 5.8:** For the covering of  $\mathbb{D}_3$ , we observe the  $i$ -th sheet of  $\tilde{\mathbb{D}}_3$  with the cuts applied across each of the three punctures. The base point of the loop is indicated by the red dot, and labelled as  $t^i \zeta$ . The power of  $t$  indicates that we are on the  $i$ -th sheet of the covering. The portions of three different loops are drawn to illustrate the behavior of loops as they pass through various edges on  $\tilde{\mathbb{D}}_{3,i}$ . The loop that would traditionally be  $x_1$  is labeled by  $t^i x_1$  to indicate that it's starting on the  $i$ -th sheet. When it passes through the left edge corresponding to this puncture labeled with a 1, it traverses up to the sheet  $\tilde{\mathbb{D}}_{3,i+1}$  and ends at base point  $t^{i+1} \zeta$ . Similarly, the loop that starts on  $\tilde{\mathbb{D}}_{3,i-1}$  and passes through the left edge of puncture 2 ends up coming out of the right edge of puncture 2 on  $\tilde{\mathbb{D}}_{3,i}$  and ends at the base point  $t^i \zeta$ . This loop is labeled by the starting sheet, so it is  $t^{i-1} x_2$ . Finally, the loop that starts on  $\tilde{\mathbb{D}}_{3,i+1}$  and passes through the right edge of puncture 3 ends up coming out of the left edge of puncture 3 on  $\tilde{\mathbb{D}}_{3,i}$ . This loop is labeled by  $-t^i x_3$  since it is the inverse of  $t^i x_3$ , with the negative sign indicating that the loop direction is reversed.

Now, viewing a single sheet, say  $\tilde{\mathbb{D}}_{n,0}$ , from above, when a loop with base point  $\tilde{\zeta}_0$  passes through a cut from the left, it traverses up to the next sheet, and ends at the base point  $\tilde{\zeta}_1$ . Similarly, a loop passing through a cut from the right ends at the base point  $\tilde{\zeta}_{-1}$ , on the sheet  $\tilde{\mathbb{D}}_{n,-1}$  below  $\tilde{\mathbb{D}}_{n,0}$ . To keep track of the various loops, we use a free parameter  $t$ . For example, a loop  $\gamma$  that starts on  $\tilde{\mathbb{D}}_{n,j}$  would be written  $t^j\gamma$ , for  $j \in \mathbb{Z}$ . Notice that the substitution of a complex number for the free parameter  $t$  results in a possibly finite degree covering. As an example, if we set  $t$  to an  $n$ -th root of unity, then we obtain an  $n$ -th degree covering of  $\mathbb{D}_n$ . For the purposes of this construction, we will keep  $t$  as a free parameter for now. Figure 5.8 demonstrates how loops interact with the cuts on different sheets. The following example describes the action of the standard generators of  $B_3$  on the covering space  $\tilde{\mathbb{D}}_3$ .

**Example 5.3.** Consider the case when  $n = 3$ . Then we have the corresponding covering space  $\tilde{\mathbb{D}}_3$  of  $\mathbb{D}_3$ . See Figure 5.8 for the view of a single sheet with various loops interacting with the cuts on the sheet. The actions of the standard generators of  $B_3$  in  $\pi_1(\mathbb{D}_3)$  are known, and can be visually understood in Figure 5.5. In the context of the covering space  $\tilde{\mathbb{D}}_3$ , the action of the generators  $\sigma_1$  and  $\sigma_2$  is observed by reducing the visualization to only the base points on each sheet and the loops themselves. This can be seen in Figure 5.9 for the case of  $\sigma_1$ .

Now, we can express loop concatenation as an abelian operation, where Eqns. 5.3–5.5 become

$$x_1 \xrightarrow{\sigma_1} x_1 + tx_2 - tx_1 = (1 - t)x_1 + tx_2, \quad (5.13)$$

$$x_2 \xrightarrow{\sigma_1} x_1, \quad (5.14)$$

$$x_3 \xrightarrow{\sigma_1} x_3. \quad (5.15)$$

Consider the vector  $\begin{bmatrix} x_1 \\ x_2 \\ x_3 \end{bmatrix}$ . Then the action of  $\sigma_1$  on the loops  $x_1, x_2, x_3$  is

realized by the matrix  $\begin{bmatrix} 1-t & t & 0 \\ 1 & 0 & 0 \\ 0 & 0 & 1 \end{bmatrix}$  since

$$\begin{bmatrix} 1-t & t & 0 \\ 1 & 0 & 0 \\ 0 & 0 & 1 \end{bmatrix} \begin{bmatrix} x_1 \\ x_2 \\ x_3 \end{bmatrix} = \begin{bmatrix} (1-t)x_1 + tx_2 \\ x_1 \\ x_3 \end{bmatrix}. \quad (5.16)$$

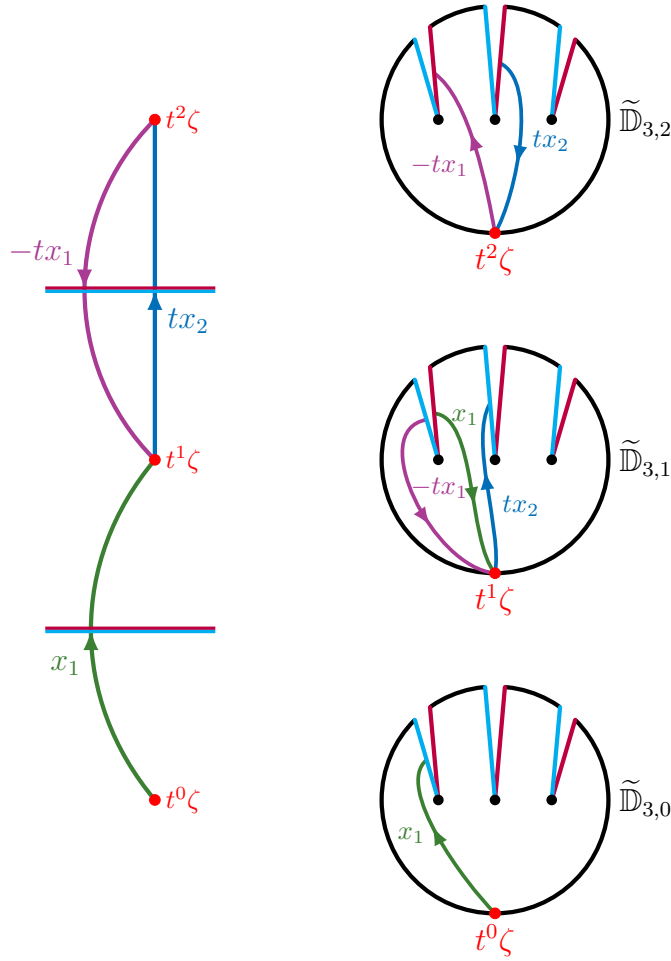


**Figure 5.9:** The loop  $\rho_{\sigma_1}(x_1) = x_1^{-1}x_2x_1$  cast onto the covering space  $\tilde{\mathbb{D}}_3$ . On the right, the loops are depicted on the corresponding sheets of the covering, and on the left is a simplified version. The order of loops is  $x_1, tx_2, -tx_1$ . The horizontal lines on the left indicate the edges taking each loop up/down a sheet.

The action of  $\sigma_2$  is obtained similarly, where

$$\sigma_2 \mapsto \begin{bmatrix} 1 & 0 & 0 \\ 0 & 1-t & t \\ 0 & 1 & 0 \end{bmatrix}. \quad (5.17)$$

Notice that these matrices have entries in the ring of Laurent polynomials,

$$\Lambda = \mathbb{Z}[t, t^{-1}].$$

The result from Example 5.3 generalizes to the case of braids on  $n$  strands. Fix  $n > 1$ . Let  $I_k$  denote the  $k \times k$  dimensional identity matrix, and let

$$U = \begin{bmatrix} 1-t & t \\ 1 & 0 \end{bmatrix}. \quad (5.18)$$

For  $i \in \{1, \dots, n-1\}$ , the action of  $\sigma_i$  on  $\pi_1(\widetilde{\mathbb{D}}_n)$  is realized as an  $n \times n$  matrix with entries in  $\Lambda = \mathbb{Z}[t, t^{-1}]$ .

The Burau representation of  $B_n$  is then defined by:

$$\psi_n : B_n \rightarrow \mathrm{GL}_n(\Lambda) \quad (5.19)$$

$$\sigma_i \mapsto \begin{bmatrix} I_{i-1} & 0 & 0 \\ 0 & U & 0 \\ 0 & 0 & I_{n-i-1} \end{bmatrix}. \quad (5.20)$$

The Burau representation need only be defined on the standard generators, since any braid  $\beta \in B_n$  decomposes into a product of  $\sigma_1, \dots, \sigma_{n-1}$  and their inverses. Notice that if we set  $t = 1$ , we recover the defining representation of  $S_n$ , as expected when we use a degree 1 covering space of  $\mathbb{D}_n$  and force the action of the generators to be abelian. Furthermore, by direct computation, it follows that

$$\psi_n(\sigma_i)\psi_n(\sigma_j) = \psi_n(\sigma_j)\psi_n(\sigma_i) \text{ for } |i-j| > 1, \quad (5.21)$$

$$\psi_n(\sigma_i)\psi_n(\sigma_{i+1})\psi_n(\sigma_i) = \psi_n(\sigma_{i+1})\psi_n(\sigma_i)\psi_n(\sigma_{i+1}) \text{ for } |i-j| = 1. \quad (5.22)$$

Moreover, the Burau representation is compatible with the natural inclusion map  $\iota : B_n \hookrightarrow B_{n+1}$  for  $n \geq 1$  and  $\beta \in B_n$ :

$$\psi_{n+1}(\iota(\beta)) = \begin{bmatrix} \psi_n(\beta) & 0 \\ 0 & 1 \end{bmatrix}. \quad (5.23)$$

## 5.7 The Reduced Burau Representation

Recall that in Section 5.4, every braid in  $B_n$  is described by an automorphism of the free group  $F_n$ . Equivalently, we thought of each generator  $\sigma_i$  as a clockwise rearrangement of adjacent punctures of  $\mathbb{D}_n$  and recorded the



resulting transformation of the  $n$  free generators of  $F_n = \pi_1(\mathbb{D}_n)$ , which were the loops around the punctures. It is intuitive to understand why the loop  $\ell = x_1 \cdots x_n$  is invariant under any braid-realized automorphism, as the loop encompasses all  $n$  punctures in  $\mathbb{D}_n$ . This was discussed in Section 5.4, and was formalized in Theorem 5.1 as a necessary and sufficient condition for the realization of braids as automorphisms on the free group.

The invariant loop  $\ell$  gives insight into the Burau representation. As was done with the generators  $x_1, \dots, x_n$  when constructing the Burau representation from  $\pi_1(\mathbb{D}_n)$ , the loop  $\ell$  is written as an element of the free  $\Lambda$ -module of rank  $n$ , denoted  $\Lambda^n$ , when cast onto the covering space  $\widetilde{\mathbb{D}}_n$ :

$$x_1 \cdots x_n \in F_n \mapsto x_1 + tx_2 + t^2x_3 + \cdots + t^{n-1}x_n = \sum_{i=1}^n t^{i-1}x_i \in \Lambda^n. \quad (5.24)$$

The right-hand side of Eqn. 5.24 manifests as a vector  $\nu = [1, t, t^2, \dots, t^{n-1}]^\top$ , where the vector components correspond to the coefficients of the free generators  $x_1, \dots, x_n$ . Note that this vector comes from the coordinate representation of  $\Lambda^n$  rather than directly from a vector space since  $\Lambda$  is not a field, but this serves as useful way to describe the elements of  $\Lambda^n$ . The coordinate description of  $\Lambda^n$  is useful in constructing a non-trivial invariant vector space with respect to the Burau representation.

In particular, notice that for any  $\sigma_i \in B_n$ , the matrix representation  $\psi_n(\sigma_i)$  leaves  $\nu$  invariant. This can be verified directly by computing the matrix

multiplication:

$$\begin{aligned}
\psi_n(\sigma_i)\nu &= \begin{bmatrix} I_{i-1} & 0 & 0 \\ 0 & U & 0 \\ 0 & 0 & I_{n-i-1} \end{bmatrix} \begin{bmatrix} 1 \\ \vdots \\ t^{i-1} \\ t^i \\ \vdots \\ t^{n-1} \end{bmatrix} \\
&= \begin{bmatrix} I_{i-1} & 0 & 0 & 0 \\ 0 & 1-t & t & 0 \\ 0 & 1 & 0 & 0 \\ 0 & 0 & 0 & I_{n-i-1} \end{bmatrix} \begin{bmatrix} 1 \\ \vdots \\ t^{i-1} \\ t^i \\ \vdots \\ t^{n-1} \end{bmatrix} \\
&= \begin{bmatrix} 1 \\ \vdots \\ t^{i-1} - t^i + t^i \\ t^i \\ \vdots \\ t^{n-1} \end{bmatrix} = \begin{bmatrix} 1 \\ \vdots \\ t^{i-1} \\ t^i \\ \vdots \\ t^{n-1} \end{bmatrix} = \nu,
\end{aligned}$$

for  $i = 1, 2, \dots, n-1$ . Since  $\nu$  is invariant under the generators of  $B_n$ , it is also invariant under any arbitrary braid in  $B_n$ . Therefore, we have a non-trivial  $\psi_n$ -invariant subspace defined by  $\text{span}\{\nu\}$ , which implies that  $\psi_n$  is reducible (provided  $n > 1$ ).

The goal of the following procedure is to obtain an irreducible representation of  $B_n$  from the Burau representation. First, given the invariance of  $\nu$  under  $\psi_n$ , we find a basis for a  $\psi_n$ -invariant vector space by looking for eigenvalues of  $\psi_n(\sigma_i)$  for  $i = 1, 2, \dots, n-1$  [3].

Let  $\mathbf{v}_i$  be defined as the vector with  $i$ -th component  $-t$ ,  $(i+1)$ -th component equal to 1, and all other components equal to zero, for  $i = 1, 2, \dots, n-1$ . Again, by direct computation, we can verify that  $\mathbf{v}_i$  is an eigenvector of

$\psi_n(\sigma_i)$  with eigenvalue  $-t$ :

$$\psi_n(\sigma_i)\mathbf{v}_i = \begin{bmatrix} I_{i-1} & 0 & 0 & 0 \\ 0 & 1-t & t & 0 \\ 0 & 1 & 0 & 0 \\ 0 & 0 & 0 & I_{n-i-1} \end{bmatrix} \begin{bmatrix} 0 \\ \vdots \\ 0 \\ -t \\ 1 \\ 0 \\ \vdots \\ 0 \end{bmatrix} = \begin{bmatrix} 0 \\ \vdots \\ 0 \\ t^2 \\ -t \\ 0 \\ \vdots \\ 0 \end{bmatrix} = -t\mathbf{v}_i.$$

**Proposition 5.2.** *Define  $\mathbf{v}_i$  as above. Then  $\text{span}\{\mathbf{v}_i\} = \text{span}\{\mathbf{v}_1, \mathbf{v}_2, \dots, \mathbf{v}_{n-1}\}$  form a non-trivial  $(n-1)$ -dimensional  $\psi_n$ -invariant vector space.*

*Proof.* The vectors  $\mathbf{v}_i$  are eigenvectors of  $\psi_n(\sigma_i)$  with eigenvalue  $-t$  for each  $i = 1, 2, \dots, n-1$ . These eigenvectors are clearly linearly independent, and so  $\text{span}\{\mathbf{v}_1, \mathbf{v}_2, \dots, \mathbf{v}_{n-1}\}$  is a non-trivial  $(n-1)$ -dimensional vector space. Clearly  $\psi_n(\sigma_i)\mathbf{v}_j = \mathbf{v}_j$  for  $|i-j| > 1$ , which is easily verified due to the block diagonal structure of  $\psi_n$ . Leveraging this block structure of  $\psi_n(\sigma_i)$  also allows the following calculations

$$\begin{aligned} \begin{bmatrix} 1 & 0 & 0 \\ 0 & 1-t & t \\ 0 & 1 & 0 \end{bmatrix} \begin{bmatrix} -t \\ 1 \\ 0 \end{bmatrix} &= \begin{bmatrix} -t \\ 1-t \\ 1 \end{bmatrix} = \begin{bmatrix} -t \\ 1 \\ 0 \end{bmatrix} + \begin{bmatrix} 0 \\ -t \\ 1 \end{bmatrix}, \\ \begin{bmatrix} 1-t & t & 0 \\ 1 & 0 & 0 \\ 0 & 0 & 1 \end{bmatrix} \begin{bmatrix} 0 \\ -t \\ 1 \end{bmatrix} &= \begin{bmatrix} -t^2 \\ 0 \\ 1 \end{bmatrix} = t \begin{bmatrix} -t \\ 1 \\ 0 \end{bmatrix} + \begin{bmatrix} 0 \\ -t \\ 1 \end{bmatrix}, \end{aligned}$$

which implies that

$$\begin{aligned} \psi_n(\sigma_i)\mathbf{v}_{i-1} &= \mathbf{v}_{i-1} + \mathbf{v}_i, \\ \psi_n(\sigma_i)\mathbf{v}_{i+1} &= -t\mathbf{v}_i + \mathbf{v}_{i+1}. \end{aligned}$$

Therefore,  $\{\mathbf{v}_1, \dots, \mathbf{v}_{n-1}\}$  are  $\psi_n(\sigma_i)$  invariant for all  $i = 1, 2, \dots, n-1$ . Hence,  $\text{span}\{\mathbf{v}_1, \dots, \mathbf{v}_{n-1}\}$  is an  $(n-1)$ -dimensional  $\psi_n$ -invariant vector space.  $\square$

We can now define the reduced Burau representation in terms of the (unreduced) Burau representation:

$$\psi_n^{\mathbf{r}} : B_n \rightarrow \mathrm{GL}_{n-1}(\Lambda) \quad (5.25)$$

$$\sigma_i \mapsto \psi_n(\sigma_i)|_{\mathrm{span}\{\mathbf{v}_i\}}. \quad (5.26)$$

In practice, we find the actual matrices for  $\psi_n^{\mathbf{r}}(\sigma_i)$  by means of a slightly different approach.

Go through derivation of  $V_i$ 's or just state it?

*not actually sure if these matrices come exactly from the same construction as above...*

*There is no widely accepted convention, and this can differ up to a matrix transposition.*

Let  $V \in \mathrm{GL}_3(\Lambda)$  be defined by

$$V = \begin{bmatrix} 1 & t & 0 \\ 0 & -t & 0 \\ 0 & 1 & 1 \end{bmatrix}. \quad (5.27)$$

Then the reduced Burau representation matrices are given by

$$\psi_n^{\mathbf{r}}(\sigma_1) = \begin{bmatrix} -t & 0 & 0 \\ 1 & 1 & 0 \\ 0 & 0 & I_{n-3} \end{bmatrix}, \quad (5.28)$$

$$\psi_n^{\mathbf{r}}(\sigma_i) = \begin{bmatrix} I_{n-2} & 0 & 0 \\ 0 & V & 0 \\ 0 & 0 & I_{n-i-2} \end{bmatrix}, \quad (5.29)$$

$$\psi_n^{\mathbf{r}}(\sigma_{n-1}) = \begin{bmatrix} I_{n-3} & 0 & 0 \\ 0 & 1 & t \\ 0 & 0 & -t \end{bmatrix}, \quad (5.30)$$

for  $i = 2, 3, \dots, n-2$  and  $n \geq 3$ .

Prove invertible?

## 5.8 Unitary Representation Matrices

As explained in [3], we can use  $U$  from the construction of the (unreduced) Burau representation to show that there are no choices of the parameter  $t$  such that the representation matrices are directly unitary. However, we can use the reduced Burau representation matrices to construct a new representation of  $B_n$  that is in fact unitary [3, 14].

First, let  $t = s^2$  for some  $s \in \mathbb{C}^*$ . In other words, we are restricting  $t$  to be a square of a nonzero complex number. Define the  $(n-1) \times (n-1)$  matrices

$$P_{n-1} = \text{diag}(s, s^2, \dots, s^{n-1}), \quad (5.31)$$

$$J_{n-1} = \begin{bmatrix} s + s^{-1} & -1 & \cdots & 0 \\ -1 & s + s^{-1} & \ddots & \vdots \\ \vdots & \ddots & \ddots & -1 \\ 0 & \cdots & -1 & s + s^{-1} \end{bmatrix}, \quad (5.32)$$

where  $\text{diag}$  denotes the diagonal matrix with the given diagonal entries. Furthermore, define  $\tilde{\psi}_n(\beta) = P_{n-1}(\psi_n^r(\beta))^\dagger (P_{n-1})^{-1}$  for  $\beta \in B_n$ . Note that

$$(P_{n-1})^{-1} = \text{diag}(s^{-1}, s^{-2}, \dots, s^{-(n-1)}).$$

Suppose that for specific choices of  $s \in \mathbb{C}^*$ , we can decompose  $J_{n-1}(s) = X^\dagger X$  for some  $(n-1) \times (n-1)$  matrix  $X$ . Then

$$(J_{n-1}(s))^\dagger = (X^\dagger X)^\dagger = X^\dagger (X^\dagger)^\dagger = X^\dagger X = J_{n-1}(s),$$

which implies that  $J_{n-1}(s)$  is Hermitian. In general,  $J_{n-1}(s)$  is Hermitian if  $s + s^{-1} \in \mathbb{R}$ . In other words, either  $s \in \mathbb{R}^*$ , or if  $s \in \mathbb{C}^*$ , then

$$\begin{aligned} s + s^{-1} = \bar{s} + \overline{s^{-1}} &\iff s + \frac{\bar{s}}{|s|^2} = \bar{s} + \frac{s}{|s|^2} \\ &\iff s - \bar{s} = \frac{s - \bar{s}}{|s|^2} \\ &\iff |s| = 1, \end{aligned}$$

where  $s\bar{s} = |s|^2$ .

Thus,  $s \in \mathbb{R}^* \cup \mathbb{C}_{|z|=1}$ , which gives a more specific description of the diagonals of  $J_{n-1}(s)$ :

$$s + s^{-1} = s + \bar{s} = 2\operatorname{Re}(s), \quad (5.33)$$

where  $\operatorname{Re}(z)$  denotes the real part of  $z \in \mathbb{C}$ . However, if  $J_{n-1}$  is to be decomposed into  $X^\dagger X$ , then we can further restrict the allowable values of  $s$ . Let  $x_{i,j}$  denote the  $(i,j)$ -th entry of  $X$ . Then it must be that

$$2\operatorname{Re}(s) = \sum_{i=1}^{n-1} \bar{x}_{i,j} x_{i,j} = \sum_{i=1}^{n-1} |x_{i,j}|^2 \geq 0,$$

for all  $j = 1, 2, \dots, n-1$ . Since  $X$  is not the zero matrix,  $\operatorname{Re}(s) > 0$ . Furthermore, we place a restriction on  $X$  by observing that

$$(X^\dagger X)_{i,j} = \sum_{k=1}^{n-1} \bar{x}_{k,i} x_{k,j} = -\delta_{i,j \pm 1},$$

where  $\delta_{ij}$  is the Kronecker delta.

For such a choice of  $s$  (hence  $X$  and  $t$ ) and any braid  $\beta \in B_n$ , the corresponding matrix

$$X \tilde{\psi}_n(\beta) X^{-1} = X P_{n-1} (\psi_n^{\mathbf{r}}(\beta))^\dagger (P_{n-1})^{-1} X^{-1} = (X P_{n-1}) (\psi_n^{\mathbf{r}}(\beta))^\dagger (X P_{n-1})^{-1}$$

is unitary.

**Example 5.4.** If  $s = e^{i\frac{\pi}{6}} = \frac{\sqrt{3}}{2} + \frac{i}{2}$ , then  $2\operatorname{Re}(s) = \sqrt{3}$ . In the  $2 \times 2$  case ( $n = 3$ ), trial and error calculations in **MATLAB** resulted in one of many possibilities for  $X$  as

$$X = \begin{bmatrix} -\frac{1}{\sqrt{2(\sqrt{2}+\sqrt{3})}} & \sqrt{\frac{1}{2}(\sqrt{2}+\sqrt{3})} \\ \sqrt{\frac{1}{2}(\sqrt{2}+\sqrt{3})} & -\frac{1}{\sqrt{2(\sqrt{2}+\sqrt{3})}} \end{bmatrix}$$

Direct computation can verify that

$$X^\dagger X = J_2(e^{i\frac{\pi}{6}}) = \begin{bmatrix} \sqrt{3} & -1 \\ -1 & \sqrt{3} \end{bmatrix}$$

Recall that  $t = s^2 = e^{i\frac{\pi}{3}}$ . The corresponding reduced Burau representation matrices are:

$$\psi_3^{\mathbf{r}}(\sigma_1) = \begin{bmatrix} -e^{i\frac{\pi}{3}} & 0 \\ 1 & 1 \end{bmatrix} \quad \text{and} \quad \psi_3^{\mathbf{r}}(\sigma_2) = \begin{bmatrix} 1 & e^{i\frac{\pi}{3}} \\ 0 & -e^{i\frac{\pi}{3}} \end{bmatrix}$$

Notice that the involution  $\eta_n : \text{GL}_n(\mathbb{C}) \rightarrow \text{GL}_n(\mathbb{C})$  defined by  $A \mapsto A^\dagger$  is an automorphism of  $\text{GL}_n(\mathbb{C})$ . Then  $\eta_2 \circ \psi_3^{\mathbf{r}}$  is a homomorphism and thus a representation of  $B_3$ . In other words, applying the hermitian adjoint to the reduced Burau representation matrices results in a new representation.

Finally, traditional conjugation of  $\eta_2 \circ \psi_3^{\mathbf{r}}$  by the matrix  $XP_{n-1}$  gives a representation  $\mathcal{U} : B_3 \rightarrow U(2)$  defined by

$$\begin{aligned} \mathcal{U}(\sigma_1) &= (XP_{n-1}) (\psi_n^{\mathbf{r}}(\sigma_1))^\dagger (XP_{n-1})^{-1} \\ &= \frac{1}{2} e^{-i\frac{\pi}{6}} \begin{bmatrix} \sqrt{3} e^{i \arctan(\frac{1}{\sqrt{2}})} & 1 \\ 1 & -\sqrt{3} e^{-i \arctan(\frac{1}{\sqrt{2}})} \end{bmatrix} \end{aligned}$$

$$\begin{aligned} \mathcal{U}(\sigma_2) &= (XP_{n-1}) (\psi_n^{\mathbf{r}}(\sigma_2))^\dagger (XP_{n-1})^{-1} \\ &= \frac{1}{2} e^{-i\frac{\pi}{6}} \begin{bmatrix} -\sqrt{3} e^{-i \arctan(\frac{1}{\sqrt{2}})} & 1 \\ 1 & \sqrt{3} e^{i \arctan(\frac{1}{\sqrt{2}})} \end{bmatrix}. \end{aligned}$$

The unitarity of  $\mathcal{U}(\sigma_1)$  and  $\mathcal{U}(\sigma_2)$  can be verified by direct computation. Additionally,  $\mathcal{U}$  satisfies the braid relation:

$$\mathcal{U}(\sigma_1)\mathcal{U}(\sigma_2)\mathcal{U}(\sigma_1) = \begin{bmatrix} 0 & i \\ i & 0 \end{bmatrix} = \mathcal{U}(\sigma_2)\mathcal{U}(\sigma_1)\mathcal{U}(\sigma_2).$$

# Chapter 6

## Anyons

### 6.1 Braiding action on a quantum system

As discussed in [4], each of the standard generators of the braid group can be realized as unitary operators on a quantum system. For the one-dimensional representations of the braid group (Section 5.5), the action on a quantum system is merely a phase shift by  $e^{ik\theta}$  for some  $\theta \in \mathbb{R}$  and  $k \in \mathbb{Z}$  the degree of the braid. We can see this explicitly by considering the action of  $\beta \in B_n$  on a wavefunction  $\psi(r_1, \dots, r_n)$  by permuting the identical particles fixed at positions  $r_1, r_2, \dots, r_n$ :

$$\psi(r_{1'}, r_{2'}, \dots, r_{n'}) = p_\theta(\beta)\psi(r_1, r_2, \dots, r_n) = e^{ik\theta}\psi(r_1, r_2, \dots, r_n),$$

where  $r_{i'}$  denotes particle  $i$ 's position after the braid  $\beta$  has been applied.

Physically, we can think of each  $\sigma_i$  as a clockwise exchange of identical particles  $i$  and  $i+1$  that live in 2 spatial dimensions. Using a third time dimension, the spacetime trajectories of the particles can be realized as a braid. In general, particles that obey the braid group permutation rules are known as *anyons* [17], and their statistics are determined by the braid group representation that describes the system.

Higher degree representations of the braid group are generally nonabelian. Thus, the action of the braid group on a quantum system will not always be as straightforward as a phase shift. This is a direct result of the “omniscience” the braid group, in the sense that a braid is only well-defined if all particle



trajectories are known. As will be investigated later, a permutation of just two anyons requires the knowledge of the positions of all other anyons in the system. These so-called *nontrivial braiding effects* of the braid group are a key feature of anyons and distinguish them from bosons and fermions.

Before studying the consequences of nontrivial braiding effects, it is instructive to first consider the action of the braid group on a quantum system with only two anyons. In Example 5.4, a 2-dimensional, nonabelian, unitary representation of  $B_3$  was constructed. Consider a degenerate set of two quantum states with orthonormal basis  $\psi_1(r_1, r_2, r_3)$  and  $\psi_2(r_1, r_2, r_3)$ . Each basis state can be thought of a column vector, written as  $|1\rangle$  and  $|2\rangle$ , for  $\psi_1$  and  $\psi_2$  respectively.

For the unitary representation  $\mathcal{U}$  constructed in Example 5.4, the action of  $\sigma_1$  on the basis states is given by

$$\begin{aligned}\mathcal{U}(\sigma_1)|1\rangle &= \frac{1}{2}e^{-i\frac{\pi}{6}}\left(\sqrt{3}e^{i\arctan(\frac{1}{\sqrt{2}})}|1\rangle + |2\rangle\right), \\ \mathcal{U}(\sigma_1)|2\rangle &= \frac{1}{2}e^{-i\frac{\pi}{6}}\left(|1\rangle - \sqrt{3}e^{-i\arctan(\frac{1}{\sqrt{2}})}|2\rangle\right).\end{aligned}$$

Similarly, the action of  $\sigma_2$  on the basis states yields

$$\begin{aligned}\mathcal{U}(\sigma_2)|1\rangle &= \frac{1}{2}e^{-i\frac{\pi}{6}}\left(-\sqrt{3}e^{-i\arctan(\frac{1}{\sqrt{2}})}|1\rangle + |2\rangle\right), \\ \mathcal{U}(\sigma_2)|2\rangle &= \frac{1}{2}e^{-i\frac{\pi}{6}}\left(|1\rangle + \sqrt{3}e^{i\arctan(\frac{1}{\sqrt{2}})}|2\rangle\right).\end{aligned}$$

As a result of this nonabelian representation, we can see that the action of the braid group on this system corresponds to nontrivial rotations in the many-particle Hilbert space that describes the quantum system [12, 4]. This differs from the one-dimensional representations of the braid group, where the action on the Hilbert space is merely a phase shift on every basis state.

More generally, if we have a set of  $m \geq 2$  degenerate states in terms of  $r_1, \dots, r_n$  with orthonormal basis  $\psi_1, \psi_2, \dots, \psi_m$ , then the basis states transform under the action of  $\sigma_k \in B_n$  as

$$\psi'_i = \sum_j [\Xi(\sigma_k)]_{ij} \psi_j,$$

where  $[\Xi(\sigma_k)]_{ij}$  is the  $(i, j)$ -th entry of the unitary matrix  $\Xi(\sigma_k)$  for some representation  $\Xi : B_n \rightarrow U(m)$ .

**Insert concluding paragraph here!** *Comment on why we care about getting the Lagrangian and Hamiltonian for anyons? In general?*

## 6.2 Two Non-Interacting Anyons

The interaction term in the Lagrangian for two anyons due to the braiding of the anyons is given by

$$\mathcal{L}_{\text{int}} = \hbar \alpha \dot{\phi}, \quad (6.1)$$

where a dot indicates a total time derivative  $\frac{d}{dt}$  and  $\phi = \arctan\left(\frac{y_2 - y_1}{x_2 - x_1}\right)$  is the relative angle between the two anyons with positions  $\mathbf{r}_1 = (x_1, y_1)$  and  $\mathbf{r}_2 = (x_2, y_2)$ . As in the previous section,  $\alpha \in [0, 1]$  is the *winding angle* or braiding statistic of the anyons. The parameter  $\alpha$  can also be thought of as an angle modulo  $\pi$ . Though the relative angle  $\phi$  is ambiguous for identical particles, the derivative  $\frac{d\phi}{dt} = \dot{\phi}$  is well-defined.

Notice that if we take  $\alpha \rightarrow 0$ , the interaction term vanishes as expected for bosons. Similarly, for  $\alpha > 0$ ,  $\phi$  becomes singular if  $\mathbf{r}_1 = \mathbf{r}_2$ , which motivates the Pauli exclusion principle for fermions. In fact, this means that for any  $\alpha > 0$ , the corresponding anyons exhibit some form of the Pauli exclusion principle.

The classical kinetic energy of this system is

$$T = \frac{1}{2}m (\dot{\mathbf{r}}_1^2 + \dot{\mathbf{r}}_2^2), \quad (6.2)$$

as expected. Then the Lagrangian for this system is

$$\mathcal{L}(\dot{\mathbf{r}}_1, \dot{\mathbf{r}}_2, \dot{\phi}) = T + \mathcal{L}_{\text{int}} = \frac{1}{2}m (\dot{\mathbf{r}}_1^2 + \dot{\mathbf{r}}_2^2) + \hbar \alpha \dot{\phi}, \quad (6.3)$$

which can also be viewed as the Lagrangian for 2 interacting bosons/fermions.

We can redefine the Lagrangian in terms of the relative and center-of-mass coordinates

$$\mathbf{R} = \frac{\mathbf{r}_1 + \mathbf{r}_2}{2}, \quad (6.4)$$

$$\mathbf{r} = \mathbf{r}_1 - \mathbf{r}_2, \quad (6.5)$$

where  $\mathbf{r}$  is the relative position vector and  $\mathbf{R}$  is the center-of-mass position vector of the two anyons. Note that we are assuming that the mass of the two particles are equal ( $m_1 = m_2$ ). Classically, the momentum of a particle is given by the product of its mass and velocity. Then the corresponding center-of-mass and relative momenta:

$$\mathbf{P} = 2m\dot{\mathbf{R}} = 2m\frac{\mathbf{r}_1 + \mathbf{r}_2}{2} = m\dot{\mathbf{r}}_1 + m\dot{\mathbf{r}}_2 = \mathbf{p}_1 + \mathbf{p}_2, \quad (6.6)$$

$$\mathbf{p} = \mu\dot{\mathbf{r}} = \frac{m}{2}(\dot{\mathbf{r}}_1 - \dot{\mathbf{r}}_2) = \frac{\mathbf{p}_1 - \mathbf{p}_2}{2}, \quad (6.7)$$

where  $m$  is the mass of each anyon and  $\mu$  is the reduced mass of the system.

With this in mind, we derive the following identity:

$$\dot{\mathbf{R}} + \frac{1}{4}\dot{\mathbf{r}} = \frac{(\dot{\mathbf{r}}_1 + \dot{\mathbf{r}}_2)^2}{4} + \frac{(\dot{\mathbf{r}}_1 - \dot{\mathbf{r}}_2)^2}{4} = \frac{\dot{\mathbf{r}}_1^2 + \dot{\mathbf{r}}_2^2}{2}. \quad (6.8)$$

Thus, the Lagrangian decomposes into relative and center-of-mass components upon making the substitution from the above identity:

$$\mathcal{L} = \underbrace{m\dot{\mathbf{R}}^2}_{\mathcal{L}_R} + \underbrace{\frac{m\dot{\mathbf{r}}^2}{4}}_{\mathcal{L}_r} + \hbar\alpha\dot{\phi}, \quad (6.9)$$

where the squared velocities indicate magnitude squared. Observe that the center-of-mass component of the Lagrangian,  $\mathcal{L}_R$ , is independent of the braiding parameter  $\alpha$ . We can further simplify the relative component of the Lagrangian,  $\mathcal{L}_r$ , by noting that we can briefly write the coordinate  $\mathbf{r}$  in polar form by representing it as a complex number  $\mathbf{r} = re^{i\phi}$ . It follows that

$$|\dot{\mathbf{r}}(r, \phi)|^2 = \left| \frac{d}{dt}\mathbf{r}(r, \phi) \right|^2 = \left| \left( \dot{r} + ir\dot{\phi} \right) e^{i\phi} \right|^2 = \dot{r}^2 + r^2\dot{\phi}^2. \quad (6.10)$$

Hence, we rewrite the relative component of the Lagrangian as

$$\mathcal{L}_r = \frac{m(\dot{r}^2 + r^2\dot{\phi}^2)}{4} + \hbar\alpha\dot{\phi}. \quad (6.11)$$

Recall that the classical relative angular momentum can be described by:

$$p_\phi = \frac{d\mathcal{L}}{d\dot{\phi}} = \frac{mr^2}{2}\dot{\phi} + \hbar\alpha. \quad (6.12)$$

Now, the Hamiltonian for this system can be constructed:

$$\begin{aligned}
\mathcal{H} &= P\dot{R} + p_r\dot{r} + p_\phi\dot{\phi} - \mathcal{L} \\
&= \frac{P^2}{4m} + \frac{p_r^2}{m} + \frac{mr^2}{4}p_\phi^2 \\
&= \frac{P^2}{4m} + \frac{p_r^2}{m} + \frac{(p_\phi - \hbar\alpha)^2}{mr^2}.
\end{aligned} \tag{6.13}$$

Once again, the center-of-mass component of the Hamiltonian is independent of  $\alpha$ , and so we can focus on the relative component of the Hamiltonian, which is

$$\mathcal{H}_r = \frac{p_r^2}{m} + \frac{(p_\phi - \hbar\alpha)^2}{mr^2}. \tag{6.14}$$

For the purposes of this work, we need not carry out to find the energy eigenstates corresponding to the quantum operator of this relative Hamiltonian. More about this is found in [10].

### 6.3 Anyons in Harmonic Potential

Placing anyons in a harmonic potential alters the Hamiltonian obtained in Section 6.2. The potential energy of a 2-anyon system is given by

$$V(\mathbf{r}_1, \mathbf{r}_2) = \frac{1}{2}m\omega^2 (\mathbf{r}_1^2 + \mathbf{r}_2^2) = m\omega^2 \left( \mathbf{R}^2 + \frac{1}{4}\mathbf{r}^2 \right), \tag{6.15}$$

where  $\omega$  is the angular frequency of the harmonic potential. We can make the same substitution as in Section 6.2 to write the potential in terms of the relative and center-of-mass coordinates. As is a recurring theme, the center-of-mass component of the potential has no dependence on the braiding parameter  $\alpha$ , and corresponds to a 2-dimensional quantum harmonic oscillator problem for a particle of mass  $2m$ .

Note that we can generalize Eqn. 6.11 (now omitting the subscript  $r$ ) to an  $N$ -anyon system in a harmonic potential by writing

$$\mathcal{L} = \sum_{i=1}^N \frac{m}{2} \dot{\mathbf{r}}_i^2 + \hbar\alpha \sum_{\substack{i=1 \\ j \neq i}}^N \dot{\phi}_{ij} - \frac{m\omega^2}{2} \sum_{i=1}^N \mathbf{r}_i^2, \tag{6.16}$$

where  $\phi_{ij} = \arctan\left(\frac{y_i - y_j}{x_i - x_j}\right)$  is the relative angle between anyons  $i$  and  $j$ . For brevity, we write  $x_{ij} = x_i - x_j$  and  $y_{ij} = y_i - y_j$  to denote the relative coordinates between the anyons.

More generally, let  $\mathbf{r}_{ij} = \mathbf{r}_i - \mathbf{r}_j$  be the relative coordinate between anyons  $i$  and  $j$ , and define  $r_{ij}^2 = |\mathbf{r}_{ij}|^2$ . Then we can solve directly for  $\dot{\phi}_{ij}$  as follows:

$$\begin{aligned}\dot{\phi}_{ij} &= \frac{d\phi_{ij}}{dt} = \frac{d}{dt} \arctan\left(\frac{y_{ij}}{x_{ij}}\right) = \frac{\frac{d}{dt}\left(\frac{y_{ij}}{x_{ij}}\right)}{1 + \left(\frac{y_{ij}}{x_{ij}}\right)^2} \\ &= \frac{x_{ij}\dot{y}_{ij} - \dot{x}_{ij}y_{ij}}{x_{ij}^2 \left[1 + \left(\frac{y_{ij}}{x_{ij}}\right)^2\right]} \\ &= \frac{x_{ij}\dot{y}_{ij} - \dot{x}_{ij}y_{ij}}{x_{ij}^2 + y_{ij}^2} \\ &= \frac{\mathbf{r}_{ij} \times \dot{\mathbf{r}}_{ij}}{r_{ij}^2}.\end{aligned}$$

Setting  $\hbar = 1$ , we can rewrite the Lagrangian as [2]

$$\mathcal{L} = \frac{m}{2} \sum_{i=1}^N [\dot{\mathbf{r}}^2 - \omega^2 \mathbf{r}_i^2] + \alpha \sum_{i < j}^N \frac{\mathbf{r}_{ij} \times \dot{\mathbf{r}}_{ij}}{r_{ij}^2}, \quad (6.17)$$

which can be expanded as

$$\mathcal{L} = \frac{m}{2} \sum_{i=1}^N [\dot{\mathbf{r}}^2 - \omega^2 \mathbf{r}_i^2] + \alpha \sum_{i < j}^N \dot{\mathbf{r}}_{ij} \cdot \frac{(-y_{ij}\hat{x} + x_{ij}\hat{y})}{r_{ij}^2}. \quad (6.18)$$

The last term in Eqn. 6.18 is of similar form to the vector (gauge) potential associated with the  $i$ -th anyon [10, 2, 11]:

$$\mathbf{A}_i(\mathbf{r}_i) = \alpha \sum_{j \neq i} \frac{\hat{z} \times \mathbf{r}_{ij}}{r_{ij}^2} = \alpha \sum_{j \neq i} \frac{-y_{ij}\hat{x} + x_{ij}\hat{y}}{r_{ij}^2}, \quad (6.19)$$

where  $\hat{z}$  is the unit vector perpendicular to the  $r_{ij}$ -plane. Here,  $\alpha$  serves as the coupling constant, which dictates the strength of the interaction between anyons in the system.

For the  $i$ -th anyon, the contribution to the Hamiltonian can be written as

$$\mathcal{H}_i = \frac{1}{2m} (\mathbf{p}_i - \mathbf{A}_i(\mathbf{r}_i))^2 + \frac{m\omega^2}{2} r_i^2, \quad (6.20)$$

where  $\mathbf{p}_i - \mathbf{A}_i(\mathbf{r}_i)$  is known as the *canonical momentum* of the system. This is a required modification since we must account for the motion of the anyons in the presence of the gauge potential in addition to their mechanical momentum.

Then, with only essential coupling between the anyons (due to the gauge potential), the Hamiltonian for the  $N$ -anyon system in a harmonic potential is given by

$$\mathcal{H} = \frac{1}{2m} \sum_{i=1}^N (\mathbf{p}_i - \mathbf{A}_i(\mathbf{r}_i))^2 + \frac{m\omega^2}{2} \sum_{i=1}^N r_i^2. \quad (6.21)$$

Substituting Eqn. 6.19 into Eqn. 6.21, we have

$$\mathcal{H} = \frac{1}{2m} \sum_{i=1}^N p_i^2 + \frac{m\omega^2}{2} \sum_{i=1}^N r_i^2 - \frac{\alpha}{2m} \sum_{\substack{i=1 \\ j \neq i}}^N \frac{\ell_{ij}}{r_{ij}^2} + \frac{\alpha^2}{2m} \sum_{\substack{i=1 \\ j, k \neq i}}^N \frac{\mathbf{r}_{ij} \cdot \mathbf{r}_{ik}}{r_{ij}^2 r_{ik}^2}, \quad (6.22)$$

where  $\ell_{ij} = (\mathbf{r}_i - \mathbf{r}_j) \times (\mathbf{p}_i - \mathbf{p}_j)$  is the relative angular momentum of anyon  $i$  and  $j$ . For details on the derivation of Eqn. 6.22, see Appendix B.

## 6.4 Nontrivial braiding effects

The last term in Eqn. 6.22 can be thought of as a long-range 2- and 3-particle interaction term. As previously established, anyons obeying braiding statistics exhibit nontrivial braiding effects. To better understand these nontrivial braiding effects, first consider two different trajectories of anyons, as depicted in Figure 6.1 [10].

From a top-down perspective, trajectory A involves a clockwise exchange of anyons 1 and 2 while anyon 3 does not take part in the exchange. In trajectory B, anyon 1 is again swapped with anyon 2 in a clockwise fashion, but anyon 3 is now involved in the exchange by being in between anyons 1

and 2. The differences between the symmetric group and the braid group now become apparent. In the symmetric group, both trajectories would be equivalent. However, the two trajectories are distinct in the braid group, which is clear by comparing the braid of each trajectory in the bottom row of Figure 6.1.

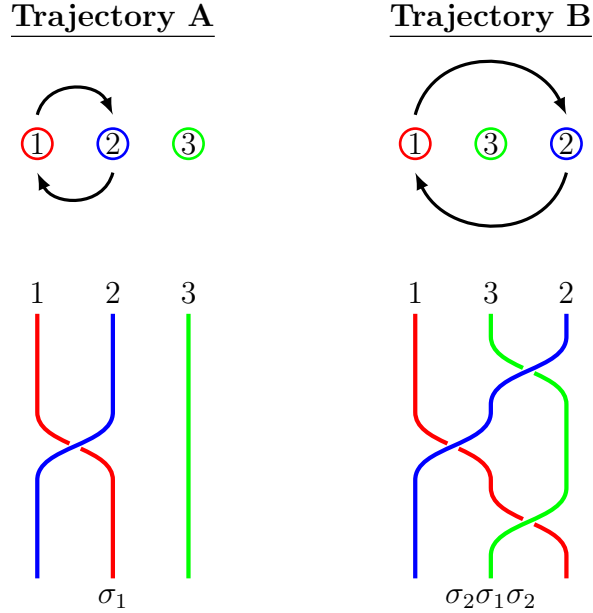


**Figure 6.1:** Two possible trajectories of three anyons viewed from above (top) and represented as braids (bottom).

Even in the one-dimensional (abelian) representation of the braid group, the nontrivial braiding effects emerge for the trajectories depicted in Figure 6.1. The braid representations for trajectory A and trajectory B are  $\sigma_1 \mapsto e^{i\theta}$  and  $\sigma_2\sigma_1\sigma_2 \mapsto e^{3i\theta}$ , respectively. As long as the choice of  $\theta$  is not an integer multiple of  $\pi$ , it follows that  $e^{i\theta} \neq e^{3i\theta}$ . This is precisely the nontrivial braiding effect.

If there were some wavefunction  $\psi(r_1, r_2, r_3)$  that described the system, then the action of the braid group on  $\psi$  would yield different phase changes for the two trajectories. Despite the fact that both trajectories involve the same exchange of anyons 1 and 2, the relative position of anyon 3 significantly impacts the outcome of the exchange. It is then evident that for a system of  $N$  anyons, every particle exchange must also simultaneously consider the

relative positions of all other anyons in the system in order to properly encode the braiding action.

Clearly, nontrivial braiding affects must be accounted for when studying a system that obeys braiding statistics. In fact, nontrivial braiding is already encoded into the Hamiltonian found Section 6.3. For a 2-anyon system, the long-range interaction term manifests in a familiar form.

Isolating the last term in Eqn. 6.22 for  $N = 2$  anyons, we see that

$$\frac{\alpha^2}{2m} \left( \frac{\mathbf{r}_{12} \cdot \mathbf{r}_{12}}{r_{12}^2 r_{12}^2} + \frac{\mathbf{r}_{21} \cdot \mathbf{r}_{21}}{r_{21}^2 r_{21}^2} \right) = \frac{\alpha^2}{mr_{12}^2},$$

which is analogous to the Coulombic interaction between two charged particles. Only when we have  $N \geq 3$  anyons will the nontrivial braiding effects truly present themselves in the long-range interaction term of the Hamiltonian. For example, if we take  $N = 3$ , the last term in Eqn. 6.22 becomes

$$\frac{\alpha^2}{m} \left( \underbrace{\frac{1}{r_{12}^2} + \frac{1}{r_{13}^2} + \frac{1}{r_{23}^2}}_{\text{Coulomb-like interaction}} + \underbrace{\frac{\mathbf{r}_{12} \cdot \mathbf{r}_{13}}{r_{12}^2 r_{13}^2} + \frac{\mathbf{r}_{21} \cdot \mathbf{r}_{23}}{r_{21}^2 r_{23}^2} + \frac{\mathbf{r}_{31} \cdot \mathbf{r}_{32}}{r_{31}^2 r_{32}^2}}_{\text{Nontrivial braiding}} \right).$$

With three anyons, the nontriviality of the long-range interaction becomes clear, as there are now cross terms that involve the relative positions of all three anyons. This result is similar to the observations made in Figure 6.1. The consequence of these three-body interaction terms is that the system is no longer separable into independent 2-anyon systems, which greatly complicates the quantum mechanics and statistical analysis of the system [10]. The nontrivial braiding effects of anyonic systems highlights the rich complexity of the braid group and its physical implications.



# Chapter 7

## To-Do List

Potential committee members:

- Anton Kaul
- Patrick Orson
- Eric Brussel
- *Rob Easton*

---

Questions for grad ed formatting

- Bold figure captions?
- Short figure captions?
- Weird matrices.

- 
- **First:** Schur's Lemmas and at least a sketch of the proof and implication for conjugacy class and irreducible representation correspondence.
  - Chapter 2 nicer notation and stray away from Tung's notation when possible.
  - Enough examples of representations?

- At least briefly discuss  $U(n)$  either here or in braid rep chapter.
- Change/modify irreducible rep. example in Chapter 2.
- Fix equation numbers

- 
- Show  $\psi_n(\sigma_i)$  invertible? Yes, eventually
  - Derive  $\psi_n^{\mathbf{r}}(\sigma_i)$  matrices or state?
  - Show  $\psi_n^{\mathbf{r}}(\sigma_i)$  invertible? Yes, eventually
  - Separate chapters into braid group and braid group reps.?

- 
- Concluding paragraph on first section of Chapter 6 to lead into the more physics-y stuff.
  - **Next?** Anyon fusion rules.  $\tau$  anyon/Fibonacci anyon example. Relate to singlet/triplet states in spin-1/2 system.
  - Spend some time on MATLAB thing?

- 
- Go over, Chapter 4 see if it needs more examples, maybe push to appendix.
  - Appendix: Gauge theory background, physics (QM) background.
  - Conclusion/future of anyons/braid group in physics.
  - Introduction “chapter”
  - Abstract
  - Title
  - Acknowledgements

---

**Format!!**

# Bibliography

- [1] E. Artin. Theory of braids. *The Annals of Mathematics*, 48(1):101, January 1947.
- [2] G. Date, M. V. N. Murthy, and Radhika Vathsan. Classical and quantum mechanics of anyons, 2003.
- [3] Colleen Delaney, Eric C. Rowell, and Zhenghan Wang. Local unitary representations of the braid group and their applications to quantum computing, 2016.
- [4] Avinash Deshmukh. An introduction to anyons.
- [5] W. Fulton. *Algebraic Topology: A First Course*. Graduate Texts in Mathematics. Springer New York, 1997.
- [6] Juan Gonzalez-Meneses. Basic results on braid groups, 2010.
- [7] David J. Griffiths and Darrell F. Schroeter. *Introduction to Quantum Mechanics*. Cambridge University Press, August 2018.
- [8] Brian C. Hall. *Quantum Theory for Mathematicians*. Springer New York, 2013.
- [9] Christian Kassel and Vladimir Turaev. *Homological Representations of the Braid Groups*, page 93–150. Springer New York, 2008.
- [10] Avinash Khare. *Fractional Statistics and Quantum Theory*. WORLD SCIENTIFIC, February 2005.
- [11] K Moriyasu. *An Elementary Primer for Gauge Theory*. WORLD SCIENTIFIC, October 1983.

- [12] Chetan Nayak, Steven H. Simon, Ady Stern, Michael Freedman, and Sankar Das Sarma. Non-abelian anyons and topological quantum computation. *Reviews of Modern Physics*, 80(3):1083–1159, September 2008.
- [13] Dale Rolfsen. Tutorial on the braid groups, 2010.
- [14] Craig C. Squier. The burau representation is unitary. *Proceedings of the American Mathematical Society*, 90(2):199–202, 1984.
- [15] Jean-Luc Thiffeault. The burau representation of the braid group and its application to dynamics. Presentation given at Topological Methods in Mathematical Physics 2022, Seminar GEOTOP-A, September 2022.
- [16] Wu-Ki Tung. *Group theory in physics: An introduction to symmetry principles, group representations, and special functions in classical and quantum physics*. World Scientific Publishing, Singapore, Singapore, January 1985.
- [17] Frank Wilczek. Quantum mechanics of fractional-spin particles. *Physical Review Letters*, 49(14):957–959, October 1982.

# Appendix A

## Physics Background

### A.1 Dirac notation

Bra-ket notation, “Hilbert space”, inner product, why unitary, why Hermitian, etc.

## A.2 Commutator Identities

$$[A, B] = -[B, A] \quad (\text{A.1})$$

$$[A, -B] = -AB + BA = -[A, B]. \quad (\text{A.2})$$

$$\begin{aligned} [A, B + C] &= A(B + C) - (B + C)A \\ &= AB + AC - BA - CA \\ &= AB - BA + AC - CA \\ &= [A, B] + [A, C]. \end{aligned} \quad (\text{A.3})$$

$$\begin{aligned} [A^2, B] &= [AA, B] \\ &= AAB - BAA \\ &= AAB - ABA + ABA - BAA \\ &= A(AB - BA) + (AB - BA)A \\ &= A[A, B] + [A, B]A. \end{aligned} \quad (\text{A.4})$$

$$\begin{aligned} [A, BC] &= ABC - BCA \\ &= ABC - BAC + BAC - BCA \\ &= (AB - BA)C + B(AC - CA). \end{aligned} \quad (\text{A.5})$$

### A.3 Commutation relations for SO(3)

$$[y, \hat{p}_y] = y\hat{p}_y - \hat{p}_y y = \cancel{y\hat{p}_y} - \overbrace{(-i\hbar + \cancel{y\hat{p}_y})}^{\text{product rule}} = i\hbar,$$

$$[\hat{L}_z, \hat{p}_z] = [x\hat{p}_y - y\hat{p}_x, \hat{p}_z] = [x\hat{p}_y, \hat{p}_z] - [y\hat{p}_x, \hat{p}_z] = 0.$$

$$[\hat{L}_z, z] = [x\hat{p}_y - y\hat{p}_x, z] = [x\hat{p}_y, z] - [y\hat{p}_x, z] = 0.$$

$$[\hat{L}_z, \hat{p}_y] = [x\hat{p}_y - y\hat{p}_x, \hat{p}_y] = \cancel{[x\hat{p}_y, \hat{p}_y]}^0 - [y\hat{p}_x, \hat{p}_y] = -y\cancel{[\hat{p}_x, \hat{p}_y]}^0 - [y, \hat{p}_y]\hat{p}_x = -i\hbar\hat{p}_x.$$

$$[\hat{L}_z, y] = [x\hat{p}_y - y\hat{p}_x, y] = [x\hat{p}_y, y] - \cancel{[y\hat{p}_x, y]}^0 = x[\hat{p}_y, y] + \cancel{[x, y]}^0\hat{p}_y = -i\hbar x.$$

### A.4 Ehrenfest's theorem and conserved quantities

Possible reference here [8]!

Suppose  $G$  is an operator on a quantum Hilbert space of states. The quantity  $\langle G \rangle$  is conserved if

$$\frac{d\langle G \rangle}{dt} = 0.$$

Recall the time-dependent Schrödinger equation

$$\hat{H}\psi = i\hbar \frac{d\psi}{dt} \implies \frac{d\psi}{dt} = \frac{1}{i\hbar} \hat{H}\psi.$$

Then if  $G$  is time-independent we have

$$\begin{aligned}
\frac{d\langle G \rangle}{dt} &= \frac{d}{dt} \langle \psi | G | \psi \rangle \\
&= \left\langle \frac{d\psi}{dt} \middle| G \middle| \psi \right\rangle + \left\langle \psi \middle| G \middle| \frac{d\psi}{dt} \right\rangle + \left\langle \psi \middle| \frac{\partial G}{\partial t} \middle| \psi \right\rangle \xrightarrow{0} \\
&= \left\langle \frac{1}{i\hbar} \hat{H} \psi \middle| G \middle| \psi \right\rangle + \left\langle \psi \middle| G \middle| \frac{1}{i\hbar} \hat{H} \psi \right\rangle \\
&= \frac{i}{\hbar} \left( \langle \hat{H} \psi | G | \psi \rangle - \langle \psi | G | \hat{H} \psi \rangle \right) \\
&= \frac{i}{\hbar} \left( \langle \psi | \hat{H}^\dagger G | \psi \rangle - \langle \psi | G \hat{H} | \psi \rangle \right) \\
&= \frac{i}{\hbar} \left( \langle \psi | \hat{H} G | \psi \rangle - \langle \psi | G \hat{H} | \psi \rangle \right) \text{ because } \hat{H} \text{ is Hermitian} \\
&= \frac{i}{\hbar} \langle \psi | (\hat{H} G - G \hat{H}) | \psi \rangle \\
&= \frac{i}{\hbar} \langle \psi | [\hat{H}, G] | \psi \rangle = 0 \iff [\hat{H}, G] = 0.
\end{aligned}$$

(linear in the second argument). (See Ehrenfest's theorem).

Thus, if  $[\hat{H}, G] = 0$ , it follows that

$$\begin{aligned}
\hat{H} G - G \hat{H} = 0 &\iff \hat{H} G = G \hat{H} \\
&\iff G^{-1} \hat{H} G = \hat{H}.
\end{aligned}$$

Therefore,  $G^{-1} \hat{H} G$  and  $\hat{H}$  share the same eigenvalues (observables), which is only true if  $\hat{H}$  is invariant under  $G$ . If  $G$  generates a group of transformations, then  $\hat{H}$  is invariant under the group of transformations generated by  $G$ . If  $G$  is unitary, this invariance is often expressed as

$$G^\dagger \hat{H} G = \hat{H}.$$

Running the argument in reverse, if  $\hat{H}$  is invariant under the transformations generated by  $G$ , then  $[\hat{H}, G] = 0$ , which, by the Ehrenfest theorem, implies that  $\langle G \rangle$  is conserved.